Determining the shear wave velocity of the Los Angeles Basin

Matthew Wong and Yuping Wang

Mark Keppel High School

Alhambra, California, 91801

March 31, 2024

Abstract

We use Rayleigh waves to determine the shear wave velocity of a portion of the Los Angeles region. Correlations were constructed for two sets of six stations aligned relatively in the north-south and east-west direction, respectively. The arrival time of surface waves was estimated between the stations which was then used to determine the group velocity for different sets of frequencies, which we plotted on a dispersion curve to visualize the velocities the wave travels at different frequencies. Lastly, the dispersion curve was converted into an estimate of the shear wave velocity as a function of depth.

Introduction

The Los Angeles Basin has millions of residents with a significant earthquake risk. It is deeper than the other basins in the region such as the San Gabriel basin and the San Fernando Basin, and has faults within the basin area and is adjacent to the San Andreas fault, which is capable of an 8+ magnitude earthquake [1]. The basin itself is composed of several sedimentary layers that enhance the level of strong-motion shaking during an earthquake [1]. The shape (mainly depth) of the basins as well as the shear strength of the sedimentary material are the important factors that control the level of amplification of ground motions from earthquakes [1]. As a proxy for the strength of the material, we use the shear-wave velocity.

To measure the shear velocity, we use Rayleigh surface waves. These waves travel along the surface of the earth between the earthquake and the receiver [2]. In the study we present here, we use Rayleigh waves generated by the cross-correlation of the seismic recordings at two stations. This method uses the ambient noise generated primarily by the ocean waves breaking on California's coast [1]. Fortunately in Los Angeles, this is a strong signal. This method obviates the need for expensive and environmentally disturbing active sources such as large vibrator trucks or explosions [3].

By cross-correlating different stations, waveforms can be detected and their travel times can be measured, which can be used to determine their velocities. Understanding the velocities of these waves is crucial to determining the level to which strong ground motions are amplified. Specifically, shear wave velocities are important because when the shear wave velocity is higher, the material is stiffer, and less ground shaking will occur. Velocity is dependent on the medium in which it travels through, and shear wave velocity is lower in soft soil than in hard soil or rock.

Method and Analysis

Open-source code was modified and used to retrieve seismic data from the cloud portion of the Southern California Earthquake Data Center (SCEDC), rather than using the webservices of a Jupyter Notebook because the latter had significant data dropouts [5]. Cross-correlation utilizes two seismic stations that are running synchronously, and enhances the seismic signals picked up by both stations over the same period. It filters unnecessary noise that will not be used, allowing us to have a clearer image when picking points on a seismogram. All seismic stations chosen for cross-correlation in this study are from the Southern California Seismic Network (SCSN). We

use the vertical component (BHZ channel) for the correlations because this channel is particularly sensitive to Rayleigh waves.

We chose 6 stations in the north-south geographical orientation and 6 stations in the east-west geographical orientation. The stations in the north-south geographical orientation are especially important because ocean waves hit southern Los Angeles from the south [], and thus these stations will pick up signals from the ocean the best. One station in the middle of all the stations aligned in a linear direction is chosen to be correlated with the other stations and act as the virtual vertical source that radiates waves to the other stations (See Figure 1 for a map showing the locations of our stations chosen). In our study, station USC was chosen as the station for both the north-south and east-west measurements. The correlation data was then filtered from 0.05-0.15 Hz, 0.15-0.25 Hz, 0.35-0.45 Hz, etc. increasing in intervals of 0.1 Hz up to 1.45-1.55 Hz to target the data for a specific range of frequencies, i.e.: the interval 0.05-0.15 Hz was used to visualize the frequency of 0.10 Hz. A seismogram is then generated to show the cross-correlation results between two stations at that frequency, and we plot those seismograms near each other on a distance vs time graph, with the source station being set at a distance of 0 meters. An example is shown in Figure 2.

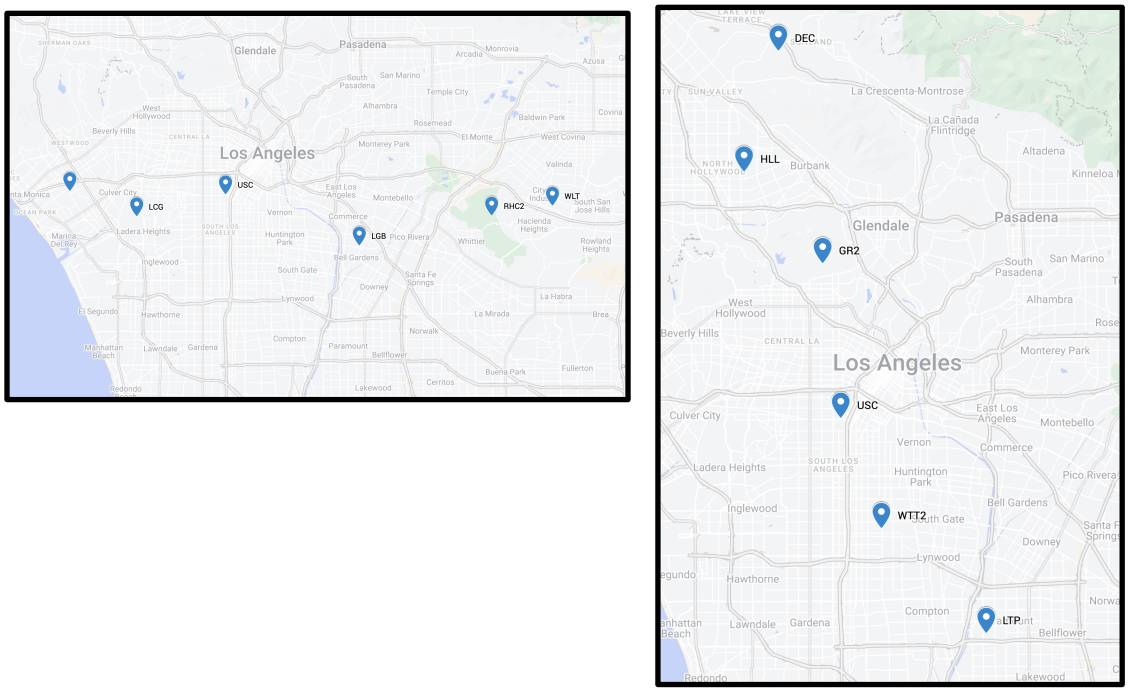

Figure 1 - Map of stations (East-West and North-South) These are maps indicating the locations of the seismometers we used for the cross-correlations. The first image details the seismometers used for the east-west correlations, while the second image details the seismometers used for the north-south correlations.

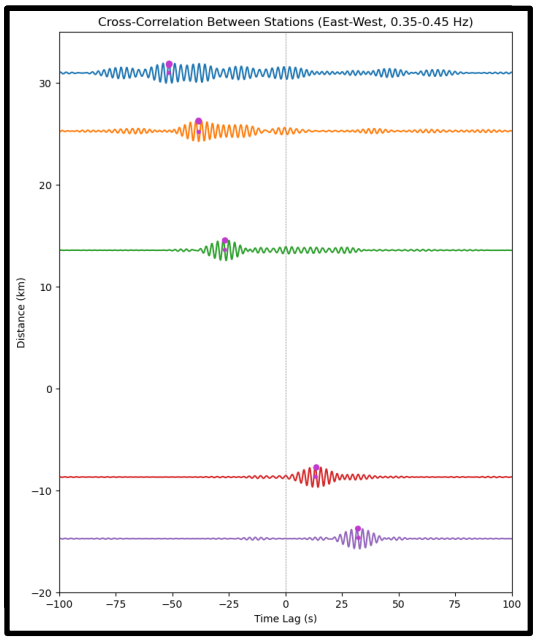

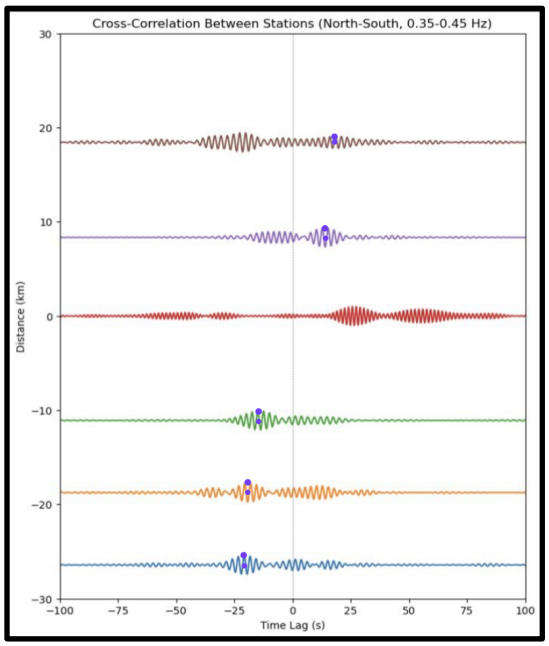

Figure 2- Correlations across stations (0.35-0.45 Hz) This is the plot of all the correlations between each of the east-west and north-south stations from 0.35-0.45 Hz. Here, we have drawn points on each of the peaks of the perturbations to visualize how we chose them. The arrival time is measured from the x-axis of the peak, and the distance between the stations is measured directly from their coordinates.

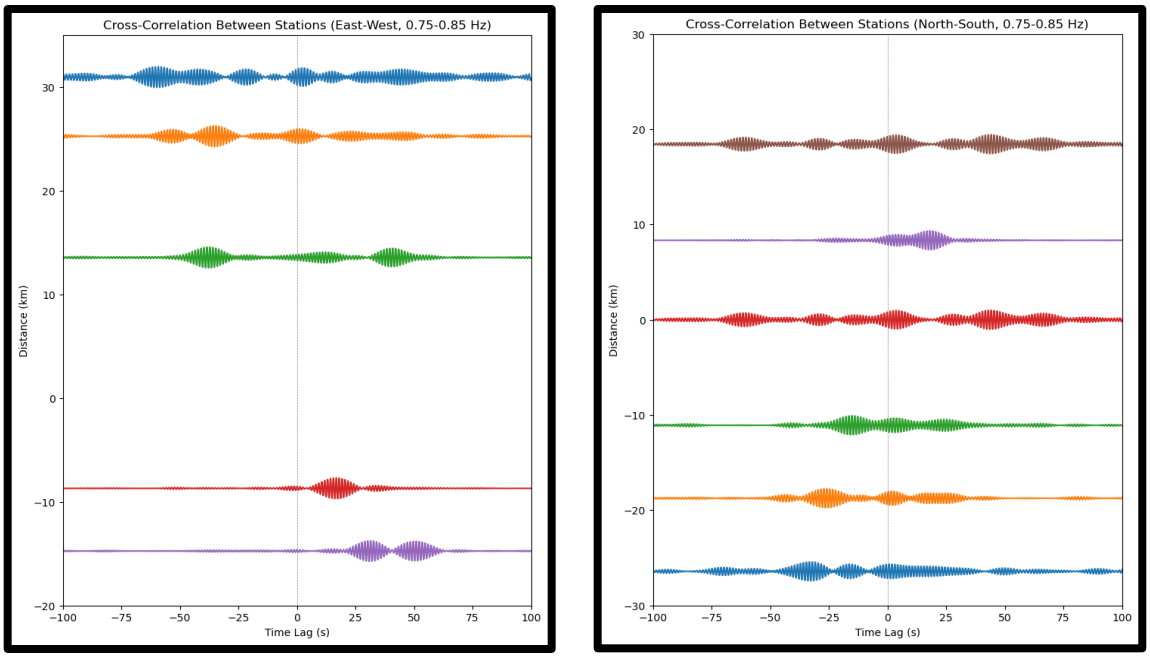

Figure 3- Correlations across stations (0.75-0.85 Hz) This is the plot of all the correlations between each of the east-west and north-south stations from 0.65-0.75 Hz, where the peaks of the arrivals are difficult to discern to because there are multiple waves at some stations. From the top to the bottom of the graph, the east-west stations were aligned from east to west geographically, while the north-south stations were aligned from north to south geographically.

This allows us to see the velocities by calculating it through the time the station sees the perturbation and the distance the station is from the source station. In frequency intervals where the perturbations were difficult to discern, the data was not used, assuming it was an outlier caused by a scattered wave. Figure 3 is below showing an example when perturbations were difficult to discern. While there is a general trend we can see, it was not enough for us to accurately pick the peaks.

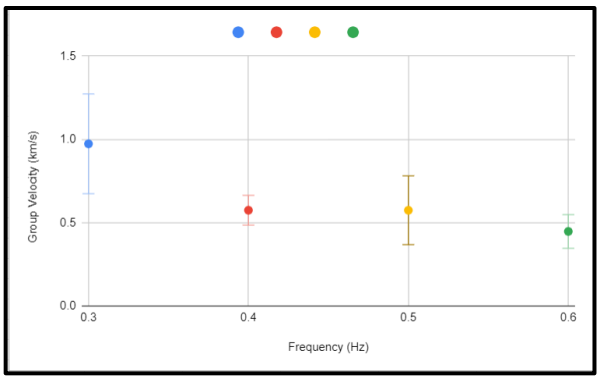

Figure 4.1- Dispersion Curve (East-West) This is the dispersion curve with the error bars plotted with the east-west stations. Each point represents a different set of correlations.

The velocities that each station had when the perturbations were received were then averaged for that specific frequency; when all the frequency sets with viable data had velocities averaged, we plotted the velocities on a velocity versus frequency graph, known as a dispersion curve, which allowed us to visualize how velocity changes as the frequency changes. The standard deviation was calculated to plot the error bars, and the dispersion curves demonstrated a downward trend, with decreasing velocities as the frequency increased. This is explained by the fact that the further down you go on Earth, the more compact the medium becomes, which decreases velocity []. Based on the equation $v = f \bullet \lambda$, because velocity is only affected by the medium in which it propagates through, wavelength decreases as you go deeper into earth, which then causes the frequency of the waves to increase.

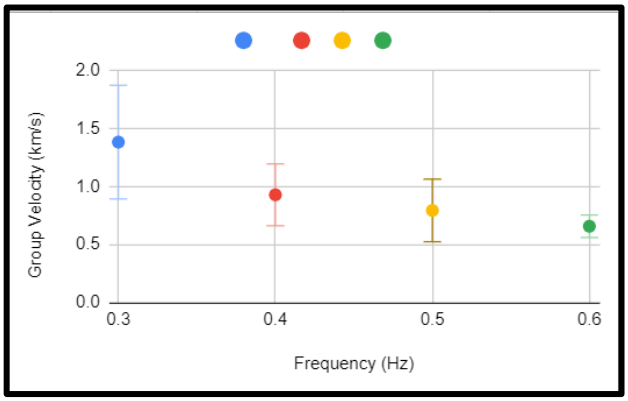

Figure 4.2- Dispersion Curve (North-South) This is the dispersion curve with the error bars plotted with the north-south stations, with each point representing a different set of correlations.

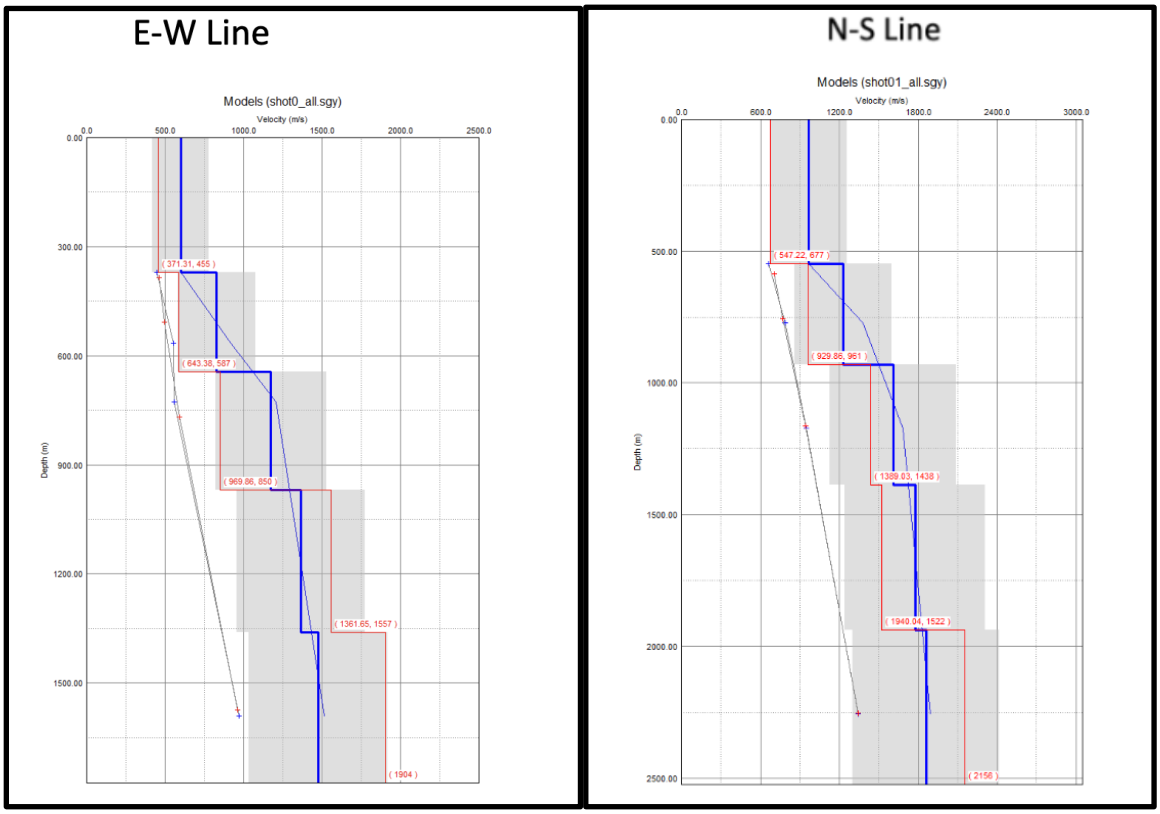

Figure 5- Phase Velocity These are the phase velocities shown for the east-west and north-south waveforms. It is shown that as the depth increases, the velocity increases as well. The blue plus-signs represents the observed trend from the dispersion curve (based on the points we picked in Figure 4) and the red plus-signs represents the modeled trend from Geogiga's software. The thicker blue line is the velocity determined from points we picked, while the red line shows velocities based on the modeled trend. The gray area shows the range of velocities that the velocity could have been or the standard deviation.

Discussions and Conclusion

Finally, the dispersion curve was transformed into a shear wave velocity versus depth graph, which shows the velocity of the wave at different depths, which was done using the "Surface" software from the Geogiga Technology Corporation [6].

To conclude, our data shows that the shear wave velocities in the Los Angeles basin travel up to around 1500 m/s in both the east-west and north-south direction when the depth exceeds about 1500 m. And as the depth increased, the velocity of the waves increased as well. In the east-west graph, the reference model's velocity was slower than the observed trend up until about 970 m in depth. Afterwards, the reference model's velocity is greater than the observed trend. For the north-south graph, the reference model's velocity was slower than the observed trend until about 1560 m in depth. Afterwards, the reference model's velocity is greater than the observed trend. We believe that these differences are simply results of the algorithm rather than an actual trend in the subsurface.

Knowing these shear wave velocities are crucial because shear wave velocities are important for site amplification of strong motion waves. We expect that when the San Andreas fault rupture occurs or when other earthquakes in southern Los Angeles happen, the shear wave velocity will be the main determining factor on the level of shaking. These results are helpful when earthquake scientists prepare for upcoming earthquakes in southern California like the long-expected San Andreas fault rupture.

Acknowledgements

The authors thank Robert Clayton of the Caltech Seismological Laboratory who provided his expertise and support with this research. The authors thanks Yan Yang and James Atterholt, both PhD students at the Caltech Seismological Laboratory, for their assistance with the code used for cross-correlating seismic stations. The authors thank Michael Gurnis of the Caltech Seismological Laboratory for introducing this research opportunity.

References

1. Schulz, S. S., & Wallace, R. E. (n.d.). The San Andreas Fault. https://pubs.usgs.gov/gip/earthq3/safaultgip.html

2. Surface Waves. Michigan Technological University. (n.d.). https://www.mtu.edu/geo/community/seismology/learn/seismology-study/surface-wave/

3. (2013, April 24). *Development of a low Cost Method to Estimate the Seismic Signature of a Geothermal Field* [Presentation]. https://www.energy.gov/eere/geothermal/articles/develpment-low-cost-method-estimate-seismic-signiture-geothemal-field

4. *Building Resonance: Structural stability during earthquakes*. Seismological Facility for the Advancement of Geoscience. (n.d.). https://www.iris.edu/hq/inclass/animation/building_resonance_the_resonant_frequency_of_different_seismic_waves

5. Hadziioannou, C., & Rijal, A. (n.d.). Seismo-Live - GitHub Pages. https://seismo-live.github.io/html/Ambient%20Seismic%20Noise/NoiseCorrelation_wrapper.html

6. *Surface*. Geogiga Technology Corp. (n.d.). https://www.geogiga.com/products/surface/

Supplementary Information

Figure S1 - Cross-correlations across stations (0.25-0.35 Hz, 0.35-0.45 Hz, 0.45-0.55 Hz,… 1.45-1.55 Hz) Below are the plots of all the correlations between each of the east-west stations from 0.25-0.35, increasing in intervals of 0.10 up to 1.45-1.55 Hz. Here, the peaks of the perturbations are difficult to discern to draw the group velocity, as there were multiple perturbations for some stations. The blue graph represents the station SMF2, orange represents LCG, green represents LGB, red represents RHC2, and purple represents WLT.

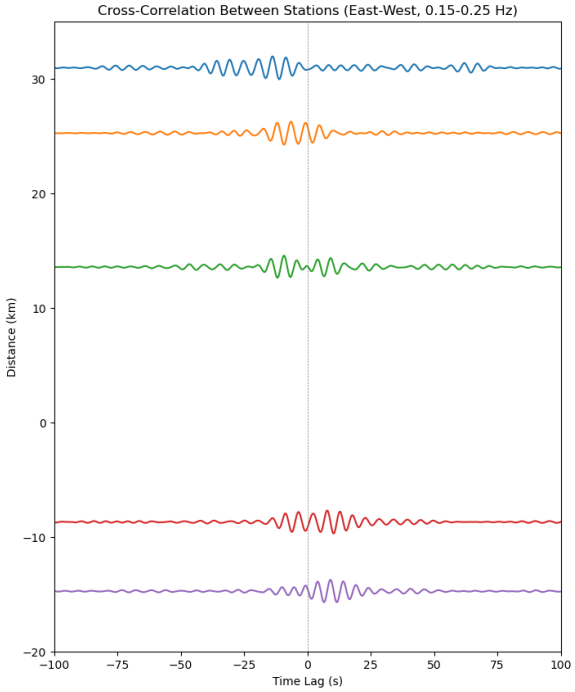
Cross-Correlation Between Stations (East-West, 0.15-0.25 Hz)
Distance (km)
Time Lag (s)
30
20
10
0
−10
−20
−100
−75
−50
−25
0
25
50
75
100

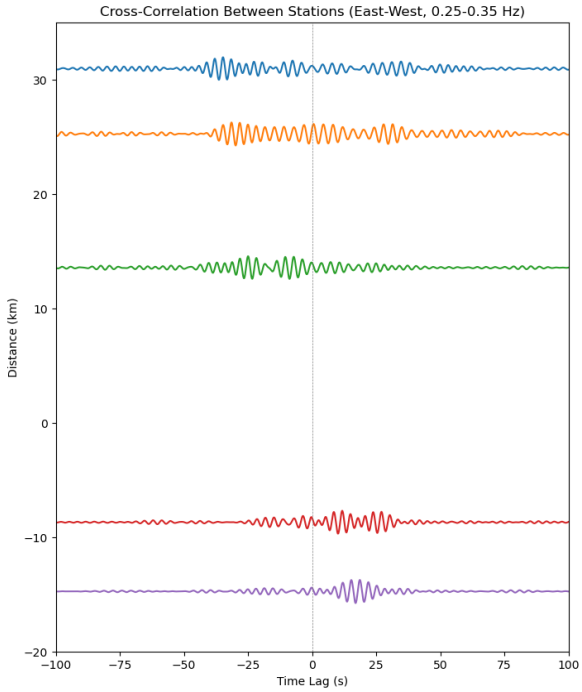
Cross-Correlation Between Stations (East-West, 0.25-0.35 Hz)
Distance (km)
Time Lag (s)
30
20
10
0
−10
−20
−100
−75
−50
−25
0
25
50
75
100

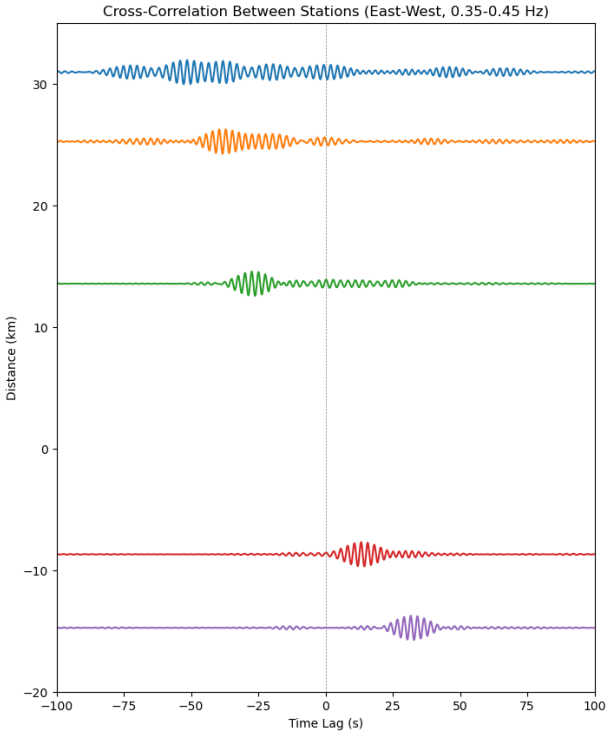
Cross-Correlation Between Stations (East-West, 0.35-0.45 Hz)
Distance (km)
Time Lag (s)

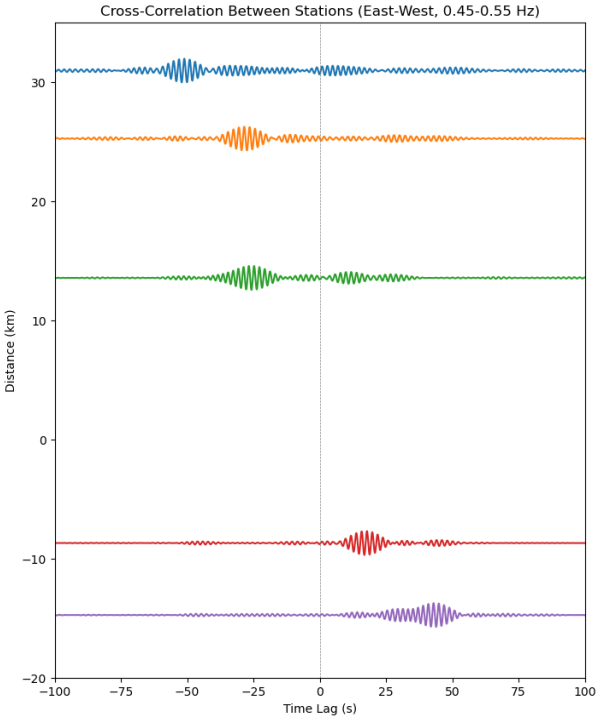
Cross-Correlation Between Stations (East-West, 0.45-0.55 Hz)
Distance (km)
Time Lag (s)

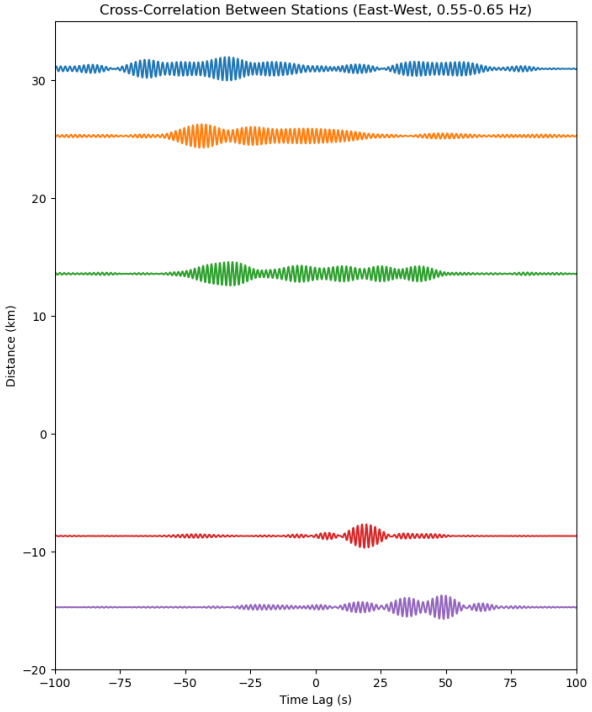
Cross-Correlation Between Stations (East-West, 0.55-0.65 Hz)
Distance (km)
Time Lag (s)

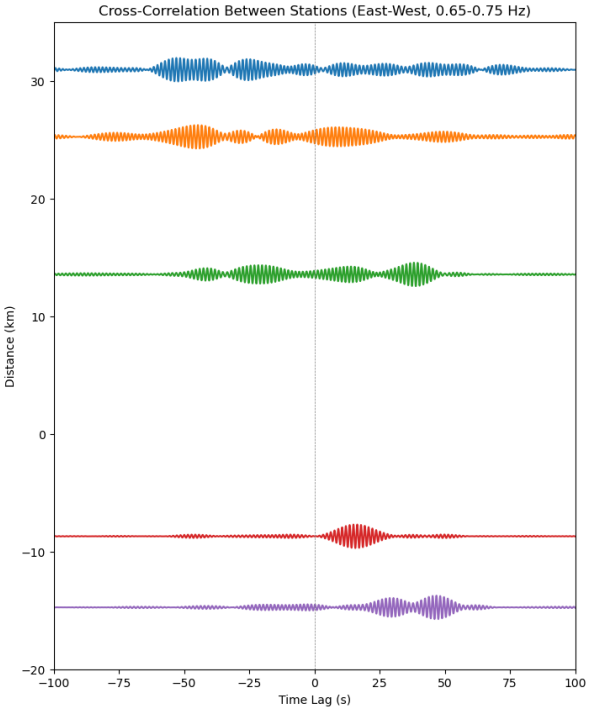
Cross-Correlation Between Stations (East-West, 0.65-0.75 Hz)
Distance (km)
Time Lag (s)

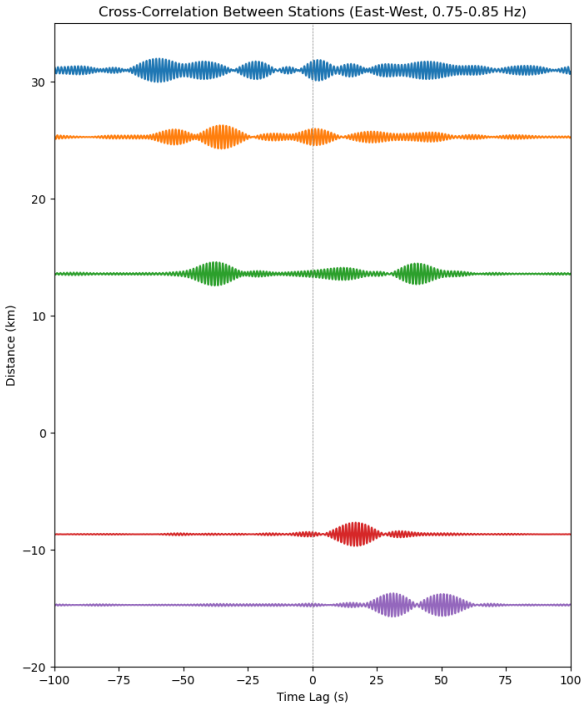
Cross-Correlation Between Stations (East-West, 0.75-0.85 Hz)
Distance (km)
Time Lag (s)

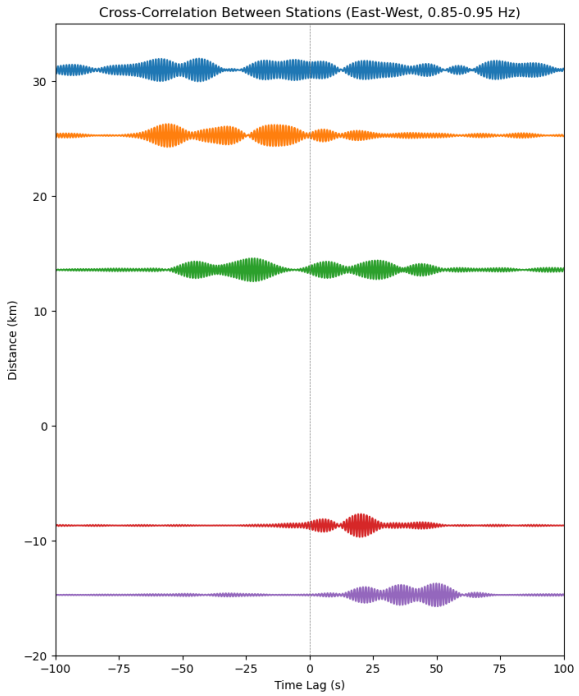
Cross-Correlation Between Stations (East-West, 0.85-0.95 Hz)
Distance (km)
Time Lag (s)

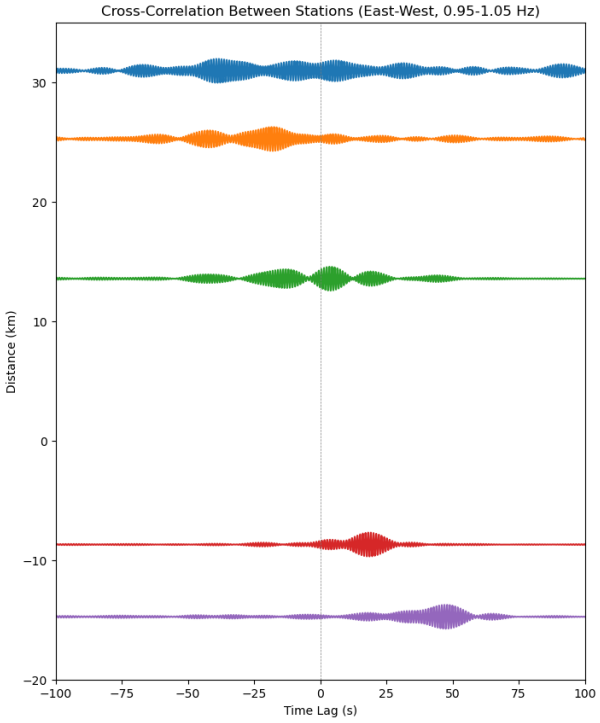
Cross-Correlation Between Stations (East-West, 0.95-1.05 Hz)
Distance (km)
Time Lag (s)

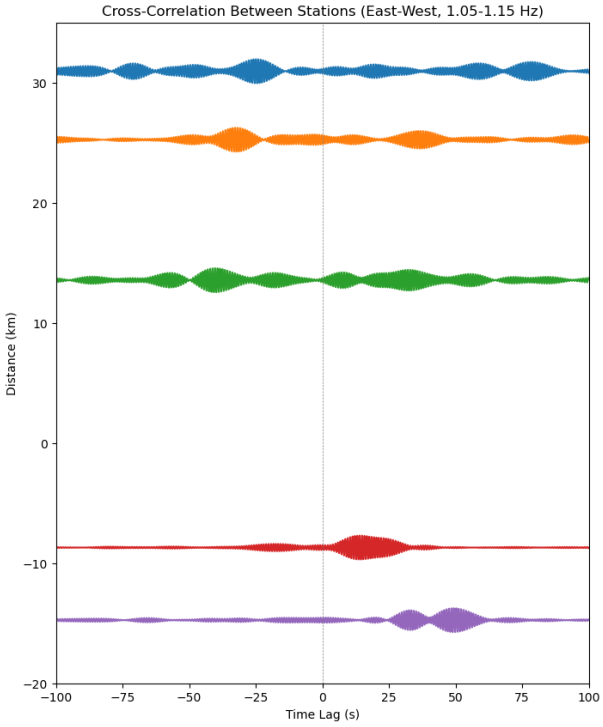
Cross-Correlation Between Stations (East-West, 1.05-1.15 Hz)
Distance (km)
Time Lag (s)

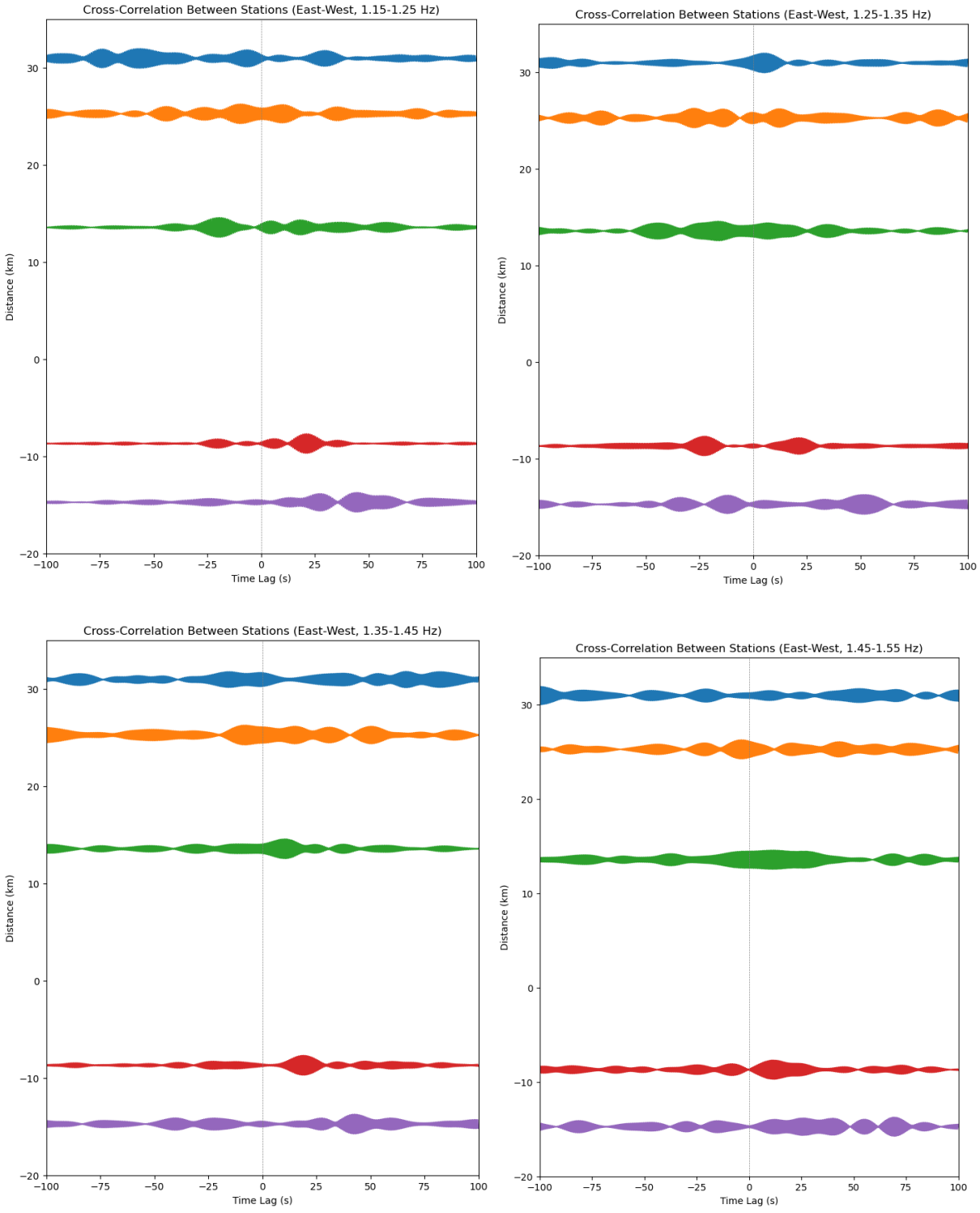

Figure S2 - Notice that for the north-south line, the peaks were picked going from the top right to the bottom left because the waveforms come from the south, and thus it takes less time for the waves to reach stations closer to the south than the north.

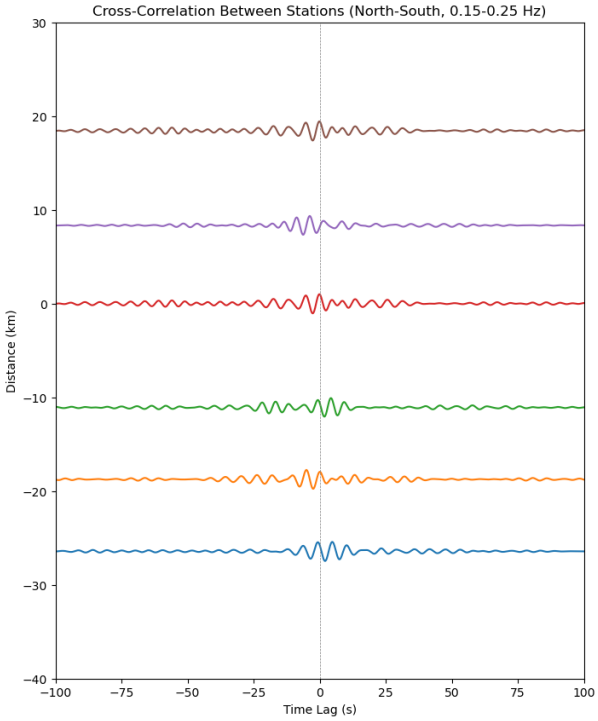
Cross-Correlation Between Stations (North-South, 0.15-0.25 Hz)
Distance (km)
Time Lag (s)

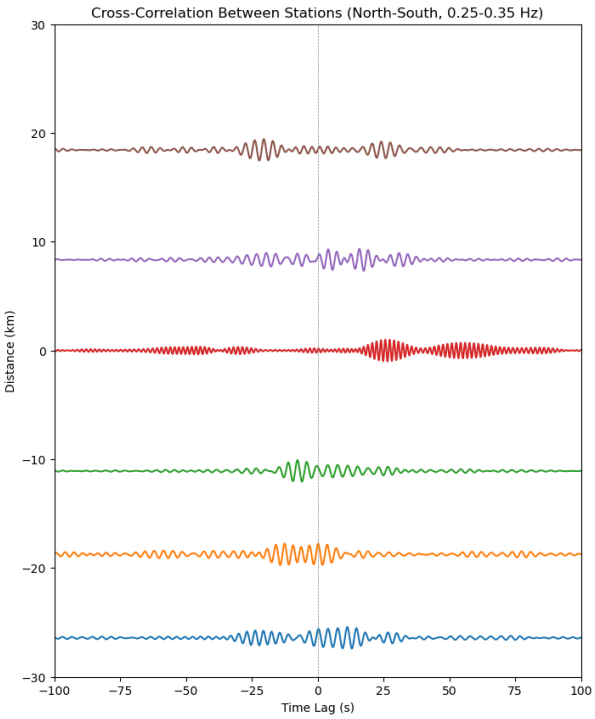
Cross-Correlation Between Stations (North-South, 0.25-0.35 Hz)
Distance (km)
Time Lag (s)

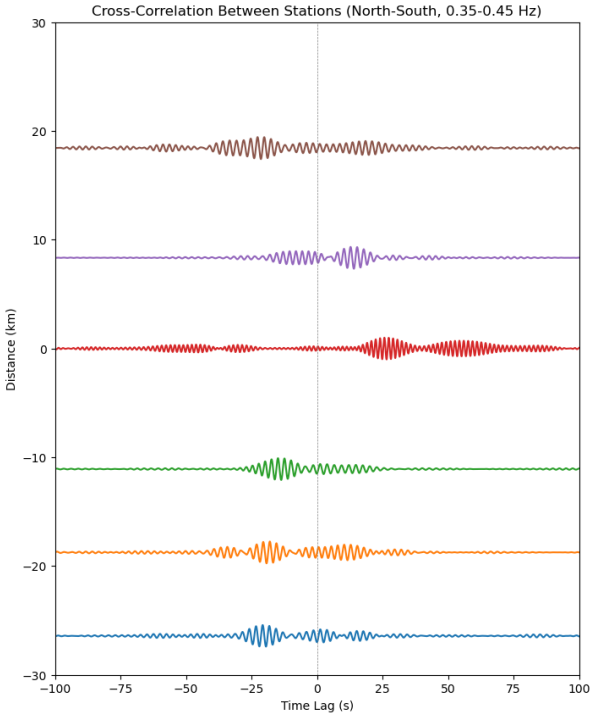
Cross-Correlation Between Stations (North-South, 0.35-0.45 Hz)
Distance (km)
Time Lag (s)

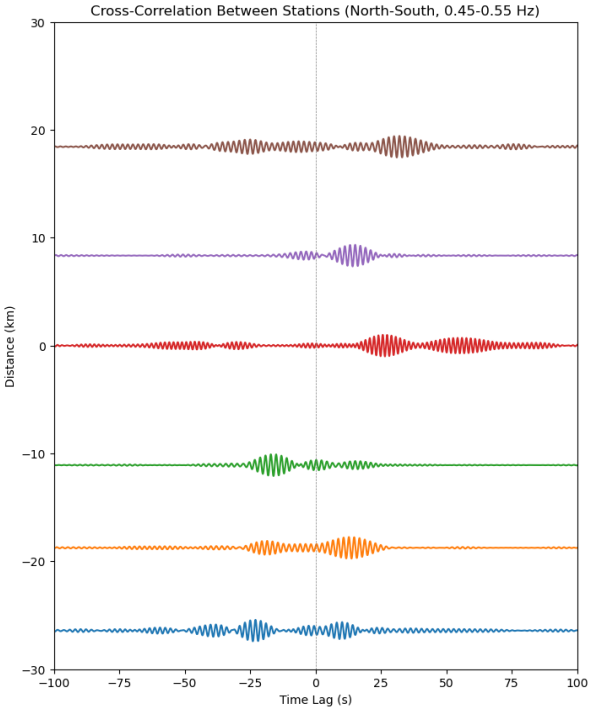
Cross-Correlation Between Stations (North-South, 0.45-0.55 Hz)
Distance (km)
Time Lag (s)

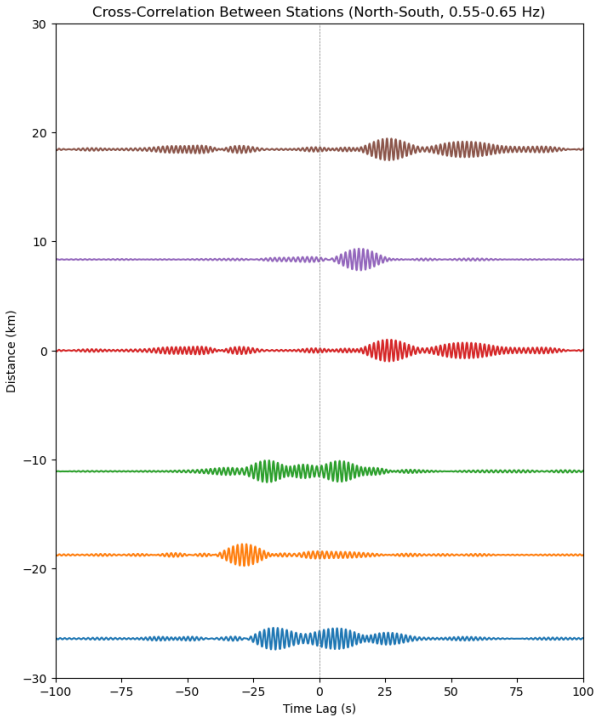
Cross-Correlation Between Stations (North-South, 0.55-0.65 Hz)
Distance (km)
Time Lag (s)
30
20
10
0
−10
−20
−30
−100
−75
−50
−25
0
25
50
75
100

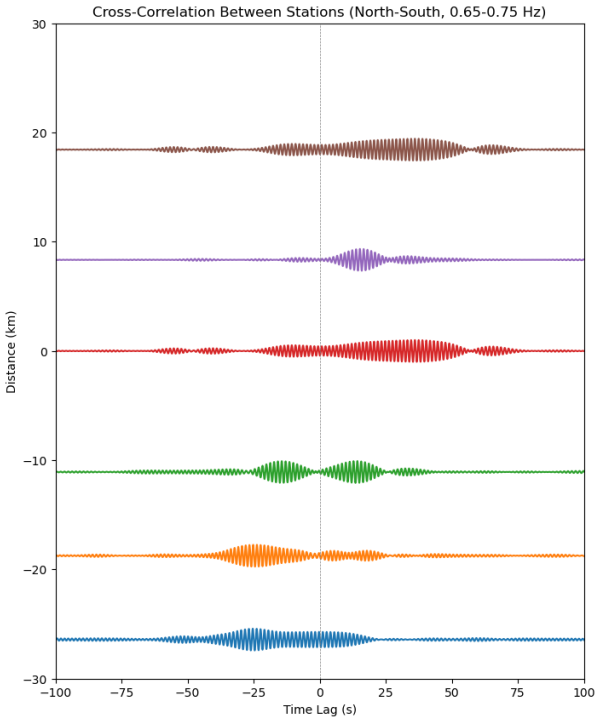
Cross-Correlation Between Stations (North-South, 0.65-0.75 Hz)
Distance (km)
Time Lag (s)
30
20
10
0
−10
−20
−30
−100
−75
−50
−25
0
25
50
75
100

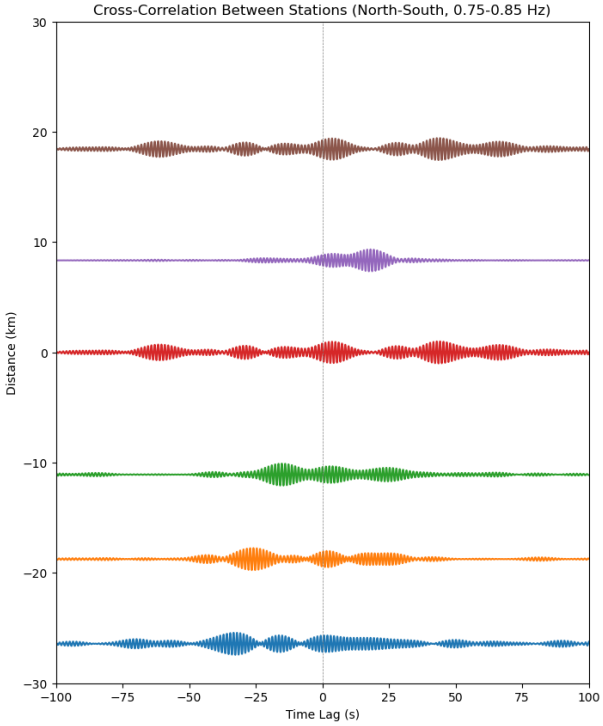
Cross-Correlation Between Stations (North-South, 0.75-0.85 Hz)
Distance (km)
Time Lag (s)
30
20
10
0
−10
−20
−30
−100
−75
−50
−25
0
25
50
75
100

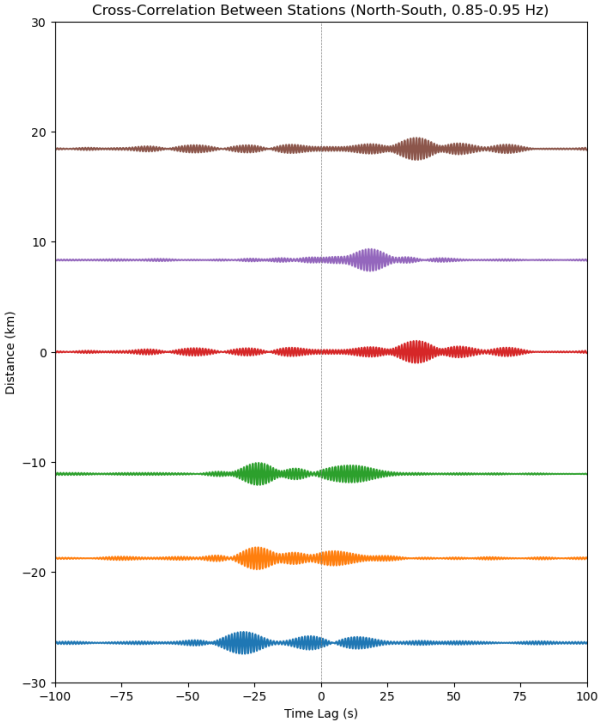
Cross-Correlation Between Stations (North-South, 0.85-0.95 Hz)
Distance (km)
Time Lag (s)
30
20
10
0
−10
−20
−30
−100
−75
−50
−25
0
25
50
75
100

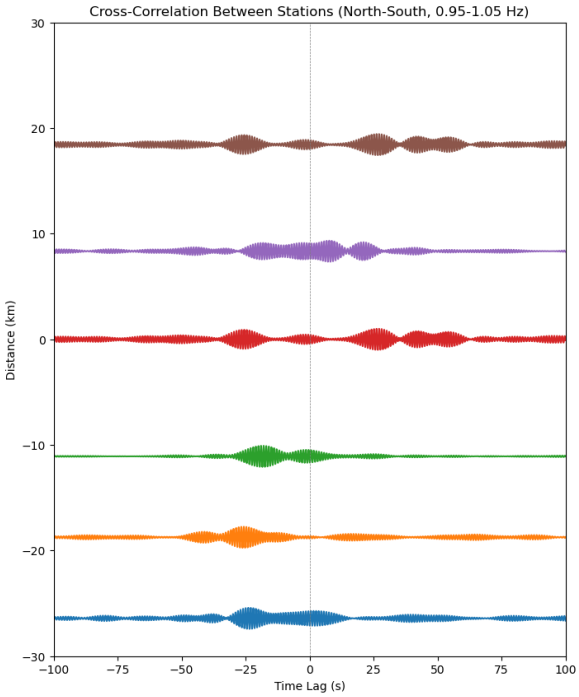

Figure S3 - Peaks picked for the north-south direction and the east-west direction correlations The chart below shows the distance and the time for each peak that we picked that forms a diagonal line based on figure S2. It also shows the average velocity and standard deviation that we used to generate the phase velocity versus depth graph in figure 5.

	(N-S line) Picked Peaks	Top right to bottom left				
Stations	**Frequency (Hz)**	**Distance (km)**	**Time (s)**	**velocity (km/s)**	**Average (km/s)**	**Standard Deviation (km/s)**
LTP	0.25-0.35	18.436	24	0.7681666667		
WTT2		8.344	4	2.086		
GR2		11.08	7.6	1.457894737	1.382889677	0.4900846294
HLL		18.744	12.6	1.487619048		
DEC		26.42	23.7	1.114767932		
LTP	0.35-0.45	18.436	18.6	0.9911827957		
WTT2		8.344	14	0.596		
GR2		11.08	15	0.7386666667	0.9287022595	0.2665698317
HLL		18.744	18	1.041333333		
DEC		26.42	20.7	1.276328502		
LTP	0.45-0.55	18.436	32	0.576125		
WTT2		8.344	15.3	0.5453594771		
GR2		11.08	16	0.6925	0.7940844128	0.2697630719
HLL		18.744	18.6	1.007741935		
DEC		26.42	23	1.148695652		
LTP	0.55-0.65	18.436	25.5	0.7229803922		
WTT2		8.344	15	0.5562666667		
GR2		11.08	19	0.5831578947	0.6577225381	0.09703403602
HLL		18.744	29.4	0.6375510204		
DEC		26.42	33.5	0.7886567164		

		(E-W line) Picked Peaks					
Stations	**Frequency (Hz)**	**Distance (km)**	**Time (s)**	**Velocity (km/s)**	**Average (km/s)**		**Standard Deviation (km/s)**
WLT		30.945	-35.1	-0.8816239316	-0.9730292919	0.9730292919	0.2994285543
RHC2		25.243	-29.9	-0.8442474916			
LGB	0.25-0.35	13.55	-9	-1.505555556			
LCG		-8.702	11	-0.7910909091			
SMF2		-14.746	17.5	-0.8426285714			
WLT		30.945	-51.5	-0.6008737864	-0.5744840409	0.5744840409	0.08926547141
RHC2		25.243	-38	-0.6642894737			
LGB	0.35-0.45	13.55	-27	-0.5018518519			
LCG		-8.702	13.5	-0.6445925926			
SMF2		-14.746	32	-0.4608125			
WLT		30.945	-51.5	-0.6008737864	-0.5742881483	0.5742881483	0.2063152955
RHC2		25.243	-28	-0.9015357143			
LGB	0.45-0.55	13.55	-26	-0.5211538462			
LCG		-8.702	17.1	-0.5088888889			
SMF2		-14.746	43.5	-0.3389885057			
WLT		30.945	-65	-0.4760769231	-0.4472244005	0.4472244005	0.1009390039
RHC2		25.243	-43.5	-0.5802988506			
LGB	0.55-0.65	13.55	-32.2	-0.4208074534			
LCG		-8.702	19	-0.458			
SMF2		-14.746	49	-0.3009387755			